Computational Modeling of Honeycomb Structures with Shape Memory Alloys

Y. Toi and J. He

Abstract— **Among many functional structures, the low shear stiffness type shape memory alloy (SMA) honeycomb structure is considered as an ideal candidate for actuator, sensor, and shape control devices. This work extends conventional SMA computational models with essential functions such as consideration of twinned martensite and enhancement for hysteresis behavior model. Using these improved models, we conducted numerical studies related to low shear stiffness type SMA honeycomb structures. Fundamental studies related to tensile and compressive loading behavior were conducted first, followed by simulation of the honeycomb core actuator considering simultaneous changes in temperature and stress level. In the field of simulation, this is the first comprehensive study related to SMA honeycomb structures. Both model validation and new discoveries could be expected from this work.**

***Index Terms*— computational mechanics, shape memory alloy, constitutive equation, honeycomb structure, honeycomb core actuator**

I. Introduction

Owing to complicated behaviors of shape memory alloy (SMA), applications of SMA actuators so far have been limited in relatively simple components, such as SMA bars, wires and beams. As the understanding of SMA's material properties are getting deeper and deeper in SMA research community, SMA applications with further complex structures have been reported from different sources. Among those reports, applications of SMA in honeycomb structures have been attracting attentions recently. Those reports include Hassan et al.[1], Michailidis et al. [2], and Okabe et al. [3]. The research on SMA honeycomb as an actuator is a major topic in this paper. To fully support simulations in SMA honeycomb actuators, we have proposed two improvements on conventional SMA computational models, focusing on SMA behaviors in low temperature environment and hysteresis environment. Implementations of this improved model include a simulation on SMA honeycomb tensile or compressive behavior, and a simulation on SMA honeycomb core actuators.

Manuscript received December 8, 2013; revised January 10, 2014.

Y. Toi is with the Institute of Industrial Science, University of Tokyo, 4-6-1 Komaba, Meguro-ku, Tokyo 153-8505, Japan (phone: 03-5452-6178; fax: 03-5452-6180; e-mail: toi@iis.u-tokyo.ac.jp).

J. He was with the Institute of Industrial Science, University of Tokyo (e-mail: jie.he@me.com)

II. Computational Model

An improved model in this paper is based on the SMA computational model proposed by Brinson [4] and Toi et al. [5]. Incremental form of stress-strain relation and phase transformation mechanism in this paper, as well as units and symbols are identical to Toi et al. [5] model.

Thermo-mechanical characteristics of SMA can be found in the temperature-stress-phase graph of Fig. 1. Three major phases exist: austenite, twinned martensite, and detwinned martensite. Other than material parameters and strain, stress σ in SMAs is mainly determined by temperature T and martensite phase fraction ξ. Incremental form of the stress-strain relationship has been developed as follows.

$$\Delta\sigma = D_{se}\left(\Delta\varepsilon + \Delta\varepsilon_{se}\right) \tag{1}$$

where $\Delta\sigma$ and $\Delta\varepsilon$ are stress and strain increments. Functions of stiffness D_{se} and $\Delta\varepsilon_{se}$ are as follows:

$$D_{se} = \frac{E}{1-\frac{dE}{d\xi}\frac{\partial\xi}{\partial\sigma}\varepsilon-\frac{d\Omega}{dE}\frac{dE}{d\xi}\frac{\partial\xi}{\partial\sigma}\xi_s-\Omega\frac{\partial\xi_s}{\partial\sigma}} \tag{2}$$

$$\Delta\varepsilon_{se} = \frac{\left[\frac{dE}{d\xi}\frac{\partial\xi}{\partial T}\varepsilon+\frac{d\Omega}{dE}\frac{dE}{d\xi}\frac{\partial\xi}{\partial T}\xi_s+\Omega\frac{\partial\xi_s}{\partial T}+\theta\right]\Delta T}{E} \tag{3}$$

where E corresponds to the elastic tensor, Ω is the phase transformation tensor, and θ is associated with the thermoelastic tensor. Martensite phase fraction ξ is divided into two parts: temperature-induced martensite fraction ξ_T and stress-induced martensite fraction ξ_S. Detailed descriptions of this model can be found in Brinson [4] and Toi et al. [5].

The temperature-stress-phase diagram of SMA is plotted in Fig. 1. This diagram shows major phase transformations in all temperature range. However, in most conventional models, only phase transformations between detwinned martensite phase and austenite phase are considered. To fill the blank in this diagram, we proposed phase transformation mechanism for phase transformation (crystallographic reorientation process) between detwinned martensite and twinned martensite. This process occurs in the environment when temperature is lower than martensite phase transformation finishing temperature, which is a possible working environment for SMA actuators.

A typical phase transformation route is marked as a vertical arrow in Fig. 1. The proposed irreversible phase transformation mechanism from twinned martensite to detwinned martensite phase is as follows:

(i) When $T < M_f$ and $\sigma_{crit.}^{start} < \frac{\sigma^{DP}}{1+\beta} < \sigma_{crit.}^{finish}$

ISBN: 978-988-19252-5-1
ISSN: 2078-0958 (Print); ISSN: 2078-0966 (Online)

$$\xi^D = \frac{1-\xi^{D0}}{2}\cos\left\{\frac{\pi}{\sigma_{crit.}^{finish}-\sigma_{crit.}^{start}}\left[\frac{\sigma^{DP}}{1+\beta}-\sigma_{crit.}^{finish}\right]\right\}+\frac{1+\xi^{D0}}{2} \quad (4)$$

To demonstrate different material properties among three phases, Young's modulus of SMA is as follows:

$$E(\xi,\xi^D) = E_A + \xi(E_M(\xi^D) - E_A) \quad (5)$$

where E is a function of the total martensite phase fraction ξ and detwinned martensite phase fraction ξ^D. Young's modulus of martensite phase E_M is:

$$E_M(\xi^D) = E_{M^T} + \xi^D(E_{M^D} - E_{M^T}) \quad (6)$$

where detwinned martensite phase fraction determines the stiffness of martensite phase E_M. E_{M^D} is the Young's modulus of the detwinned martensite phase, E_{M^T} is the Young's modulus of the twinned martensite phase.

Experimental result supported our model. An SMA ribbon with 100% initial martensite phase was tested in Hassan's work[1]. In this experiment, the martensite phase transformation finish temperature M_f is 30°C, and room temperature is 25°C. Full phase transformation (re-orientation) from twinned martensite phase to detwinned martensite phase occurred in this test. Good fitting can be observed in Fig. 2.

The second improvement is focusing on simulation stability in hysteresis environment. This improvement solved the instability problem we met in simulation on SMA honeycomb core actuators. Conventional models work well on isostress and isothermal simulations. But in stress and temperature simultaneously changing environment, hysteresis behavior may generate unpredictable results, such as non-convergence. As we can see in Fig. 3, stress-temperature route in phase transformation is unpredictable, and SMA phase transformation is a one-way process. Phase volume fraction is not only determined by its position in Fig. 1, but also the route history. Attempt to avoid instability can be found in Bekker et al. [6], who used linear distance from the phase transformation critical stress line σ_{M_s} and σ_{A_s} as the criterion to determine whether phase transformation takes place. However, for further complex model in Toi et al. [5], it is no longer applicable.

Following the train of thought by Bekker [6], we proposed two phase transformation conditions instead of Bekker's condition. One is to force phase volume fraction definition. For the area circled by blue line in Fig. 4, SMA is forced to be 100% martensite. For the area circled by red line, SMA is forced to be 100% austenite.

Another one is a special rule for phase transformation. Its mathematical expression is as follows:

- Martensite phase transformation (small figure inside Fig. 3)

$$\sigma^{DP} \geq \sigma_0^{DP} \quad (7)$$

$$T \leq T_0 \quad (8)$$

- Austenite phase transformation

$$\sigma^{DP} \leq \sigma_0^{DP} \quad (9)$$

$$T \geq T_0 \quad (10)$$

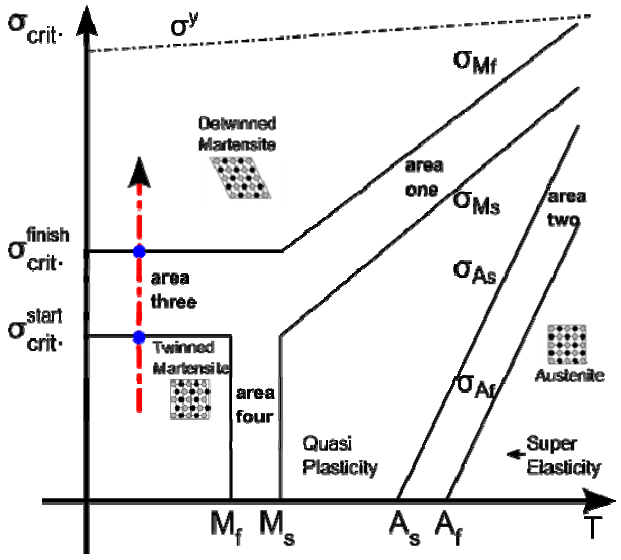

Fig. 1 Stress-temperature phase diagram

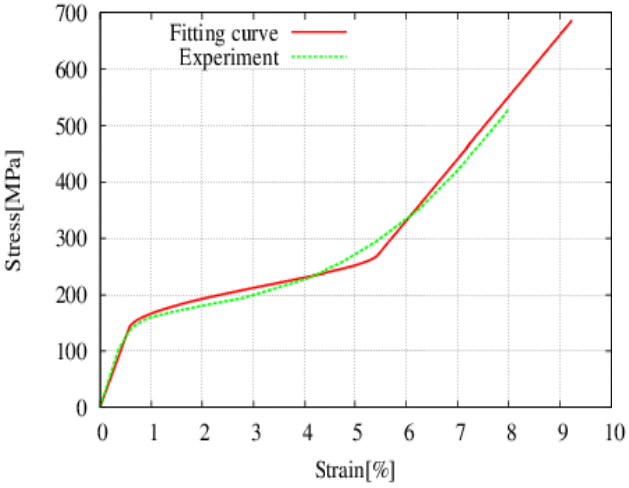

Fig. 2 Stress-strain relationship of SMA at low temperatures

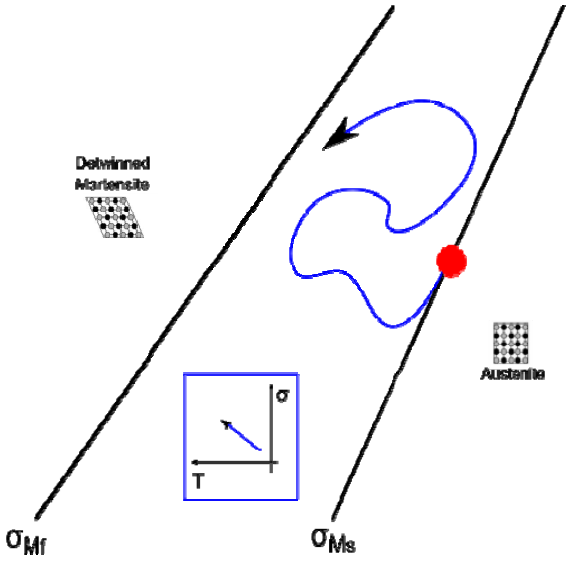

Fig. 3 Possible stress-temperature route of SMAs during martensite phase transformation

ISBN: 978-988-19252-5-1
ISSN: 2078-0958 (Print); ISSN: 2078-0966 (Online)

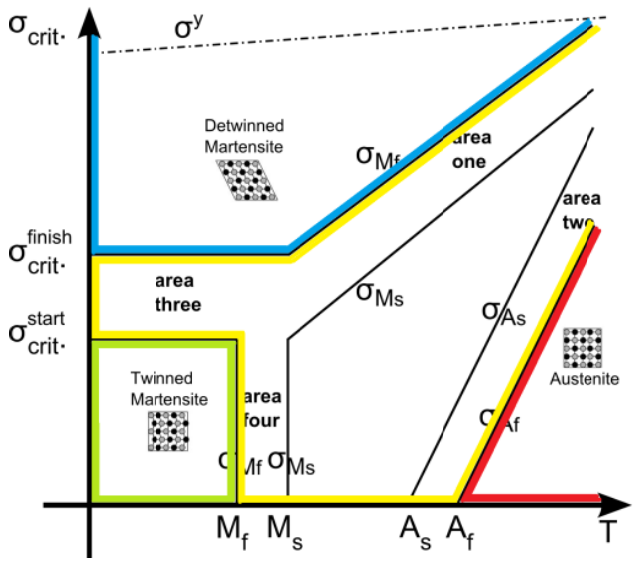

Fig. 4 Stress-temperature-phase diagram emphasizing phase transformation condition

Applications of the above-mentioned two improvements will be discussed in next section.

In all simulations in this paper, the Euler-Bernoulli cubic beam element and the beam layered approach are adopted. Beam elements in these simulations are subdivided into ten equal layers along the vertical. Each layer contains two Gaussian points. By using the layered beam approach stress, we can obtain very detailed strain and martensite phase distribution along the radial direction. In plots of following simulations, stress and martensite phase volume fraction distributions use the value of Gaussian point with maximum value in each element.

III. Numerical Studies

A. Simulation on SMA honeycomb structure behavior under tensile loading

This simulation is about a full cycle tensile loading of OX type honeycomb structure. Initial shape with its boundary condition (Fig. 5) is based on Hassan's report [1], in which loading only experiment was conducted. Martensite phase transformation finishing temperature is 30°C. Environment temperature is 25°C. Initial phase is 100% twinned martensite phase.

One-way phase transformation occurs during loading process. The average stress-strain relation during the whole cycle can be found in Fig. 6. Stiffness hardening during loading process is very similar to that of experiment, which can be considered as a qualitative validation for this simulation.

Interesting behavior can be found during unloading. After maximum displacement in Fig. 7 when maximum loading force is applied, honeycomb shows different unloading behavior (Fig. 8) other than that during loading process.

In unloading process, further deformation occurred, together with further phase transformation and cell deformation. After extensive investigation for different SMA materials, and in different temperature, we found this localized deformation behavior is an intrinsic property of SMA OX type honeycomb. Tensile loading induced X-shaped stress concentration in the honeycomb. High stress level in those area induced further phase transformation and stiffness weakening, which is the key reason of the localized deformation behavior.

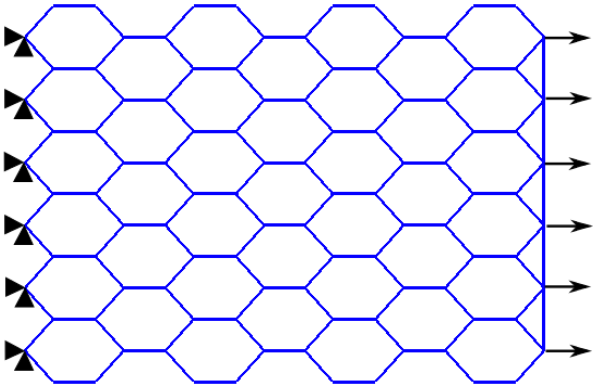

Fig. 5 Initial shape and boundary condition of OX type honeycomb structure under tensile loading

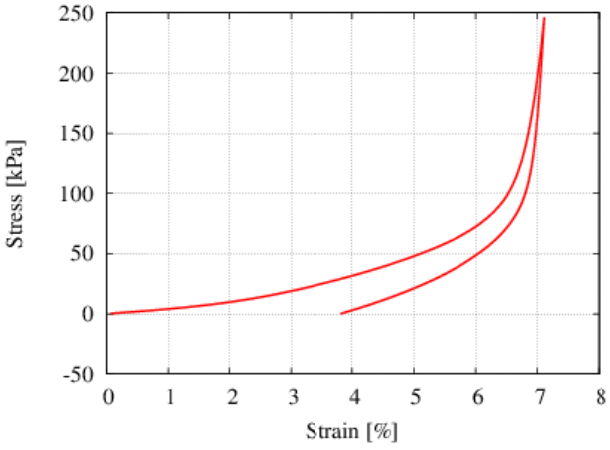

Fig. 6 Average stress-strain relationship under tensile loading

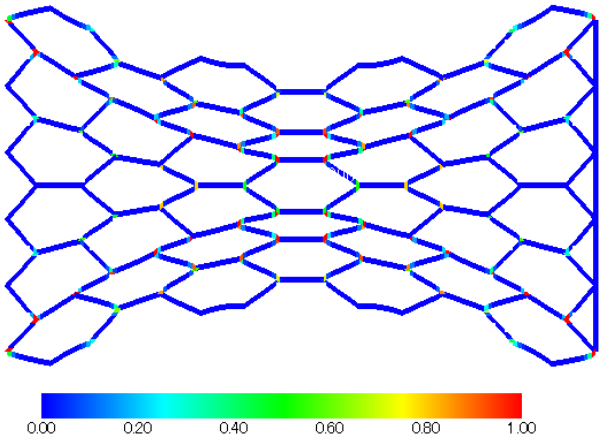

Fig. 7 Shape of OX type honeycomb structure and detwinned martensite phase fraction distribution under maximum tensile loading

ISBN: 978-988-19252-5-1
ISSN: 2078-0958 (Print); ISSN: 2078-0966 (Online)

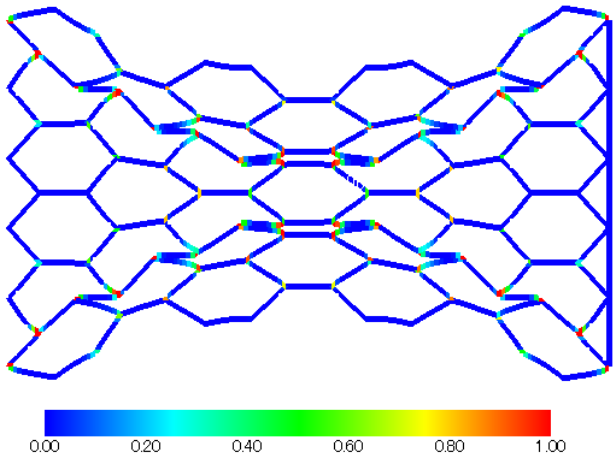

Fig. 8 Shape of OX type honeycomb structure and detwinned martensite phase fraction distribution after unloading

B. Simulation on SMA honeycomb structure behavior under compressive loading

A major difference between OX type and auxetic type honeycombs is the cell internal angle. This difference imparts several special features to auxetic-type honeycombs. A negative Poisson ratio is one example. Localized deformation in OX type honeycombs is not obvious either. These behaviors are reproduced in the following simulations.

In compressive behavior simulation, the influences of structural imperfection on structure stiffness and stability have been considered. Based on random dislocation of cell joints, the following three variants of the auxetic type structure have been generated: perfect, 1% imperfect, and 10% imperfect. The initial shapes and boundary conditions of the auxetic type honeycomb structures are shown in Fig. 9 [2]. The bottom layer of the structure is fixed in all directions. Compression forces are applied on the top layer. The whole process involves a full loading and unloading cycle.

According to the average stress-strain simulation results shown in Fig. 10, no obvious instability was observed in imperfect honeycombs. However, stiffness weakening was observed for the 1% imperfect and the 10% imperfect honeycombs.

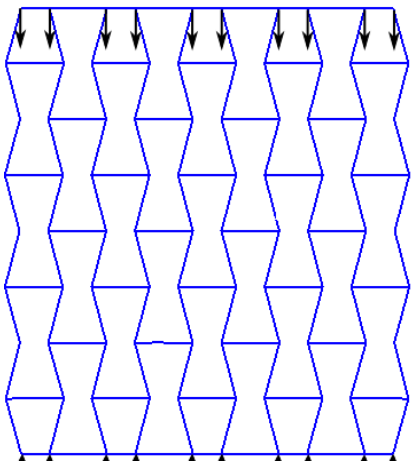

Fig. 9 Initial shape of auxetic type honeycomb structure: perfect (left), 1

Fig. 11 contains the shape and martensite phase fraction graph under maximum loading.

Fig. 12 shows the shape and martensite phase fraction graph after unloading. Owing to superelasticity, the martensite phase recovered back to the austenite phase after unloading, with minor residual martensite phase.

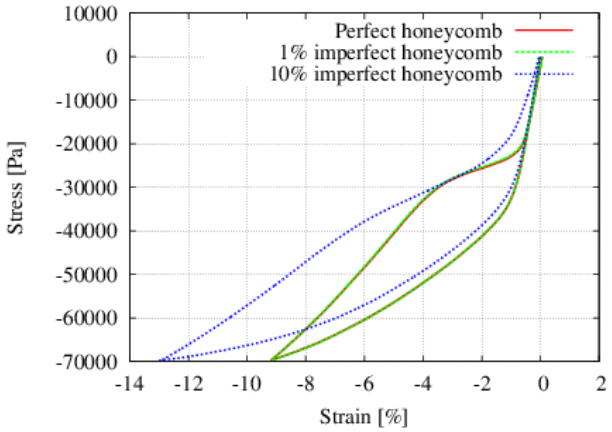

Fig. 10 Auxetic type honeycomb structure compressive behavior: average stress-strain curve

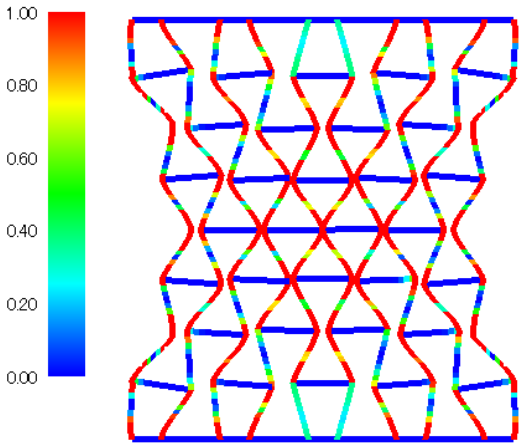

Fig. 11 Auxetic type honeycomb structure's martensite phase distribution (unit: 1) under maximum loading: perfect honeycomb structure (left),

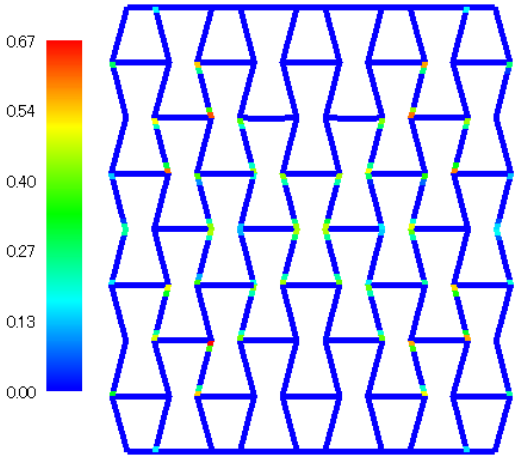

Fig. 12 Auxetic type honeycomb structure's martensite phase distribution (unit: 1) after unloading: perfect honeycomb structure (left),

ISBN: 978-988-19252-5-1
ISSN: 2078-0958 (Print); ISSN: 2078-0966 (Online)

C. Simulation on SMA honeycomb core actuator

Simulation on SMA honeycomb core actuators is based on the SMA actuator proposed by Okabe et al. [3]. This simulation uses identical set of material parameters as in experiment.

The actuating process includes two steps: step one is forced deformation process, step two is heating process. Details are plotted in Fig. 13.

In step one, the lower CFRP layer is fixed. Leftward forced displacement is applied on the upper CFRP layer. The environment temperature is 25°C, which is between martensite phase transformation start temperature and reverse phase transformation finish temperature. Detailed shape deformation and martensite phase volume fraction distribution are plotted in Fig. 14. Maximum 72% of martensite volume fraction is generated in this step.

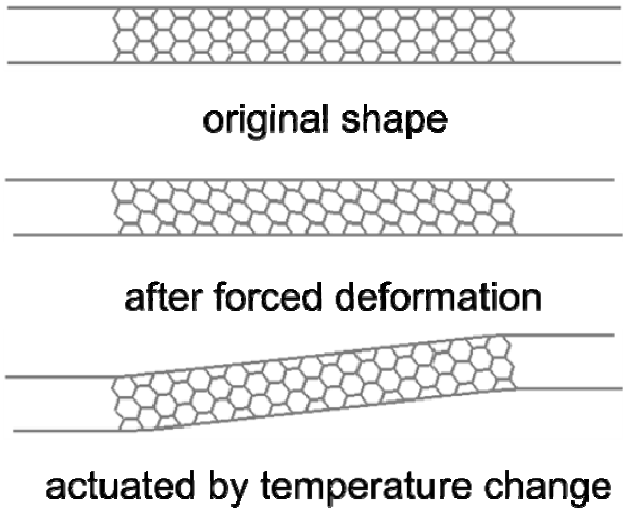

Fig. 13 Actuation process for honeycomb core actuator: step 0 -> step 1 -> step 2

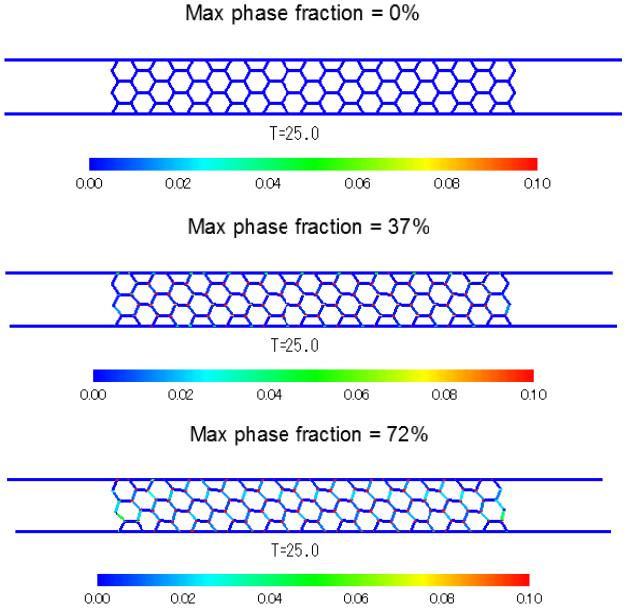

Fig. 14 Martensite phase distribution under shear force deformation (unit: 1): displacement at 0.0, 1.25, and 2.5 mm

In step two, fixation on lower CFRP layer was replaced by fixation on two ends of this actuator in horizontal direction. Temperature rises from 25°C to 80°C during this process. Higher temperature induced reverse phase transformation, which becomes the key factor of actuating. As we can see in Fig. 15, which is shape deformation and martensite phase volume fraction distribution graphs in different temperature, when temperature reaches 80°C, most martensite phases have been transformed back to austenite phase. Vertical Actuating has been achieved.

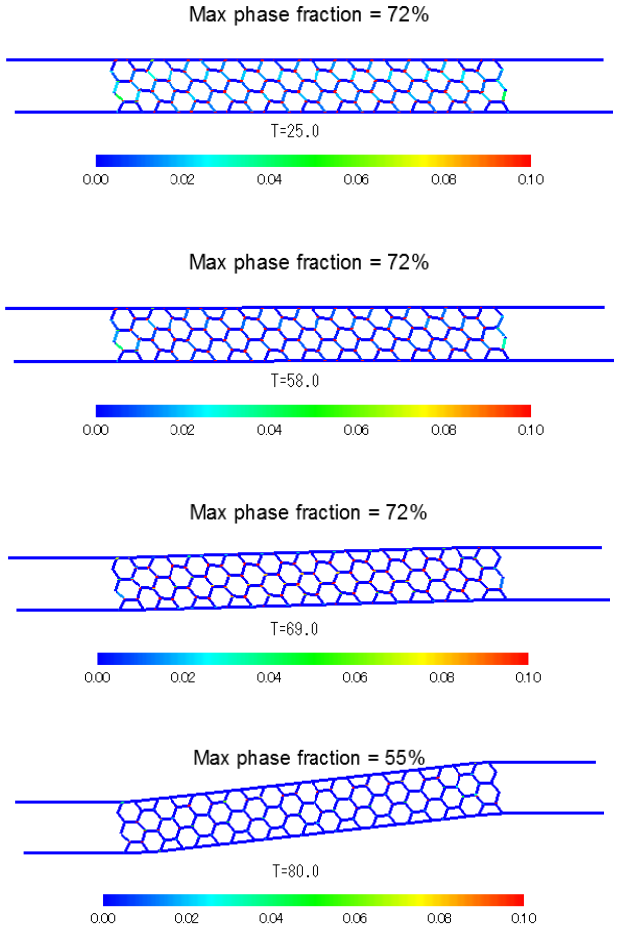

Fig. 15 Martensite phase fraction distribution during heating process (unit: 1)

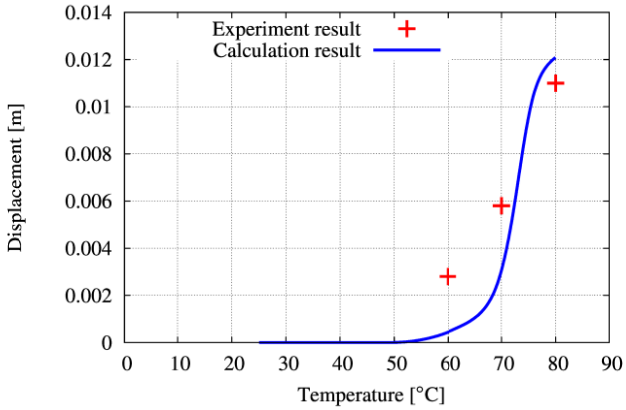

Fig. 16 Honeycomb core structure temperature-displacement curve: experimental [3] vs. simulated

ISBN: 978-988-19252-5-1
ISSN: 2078-0958 (Print); ISSN: 2078-0966 (Online)

In Fig. 16, comparison between simulation and experimental result has been provided. By using special treatment in phase transformation condition, we successfully avoided instability during SMA actuator simulation. This simulation proved the validity of this new model.

IV. Conclusion

Two improvements to conventional SMA computational models have been introduced in this paper. One is twinned martensite phase support for SMA simulation in low temperature. Another is special treatment in phase transformation condition for SMA simulation in hysteresis environment. Both improvements are essential for SMA actuator simulations. Three successful numerical examples including SMA honeycomb structure tensile/compressive behavior and SMA honeycomb core actuator proved the validity of those improvements with additional physical findings. Further implementations of the new model are expected.

References

[1] M. R. Hassan et al., "In-plane tensile behavior of shape memory alloy honeycombs with positive and negative Poisson's ratio". *Journal of Intelligent Material Systems and Structures*, vol.20, no.8, pp. 897-905, 2009..

[2] P. A. Michailidis et al., "Superelasticity and stability of a shape memory alloy hexagonal honeycomb under in-plane compression", *International Journal of Solids and Structures*, vol.46, no.13, pp. 2724-2738, 2009.

[3] Y. Okabe. et al., "Lightweight actuator structure with SMA honeycomb core and CFRP skins", *Journal of Mechanical Design*, vol.133, pp. 011006, 2011.

[4] L. Brinson, "One-dimensional constitutive behavior of shape memory alloys: thermomechanical derivation with non-constant material functions and redefined martensite internal variable", *Journal of intelligent material systems and structures,* vol.4, no.2, pp.229-242, 1993.

[5] Y. Toi et al., "Finite element analysis of superelastic, large deformation behavior of shape memory alloy helical spring", *Computers and Structures*, vol.82, no.20, pp. 1685-1693, 2004.

[6] A. Bekker and L. C. Brinson, "Temperature-induced phase transformation in a shape memory alloy: phase diagram based kinetics approach", *Journal of the Mechanics and Physics of Solids,* vol.45, no.6, pp. 949-988, 1997.

ISBN: 978-988-19252-5-1
ISSN: 2078-0958 (Print); ISSN: 2078-0966 (Online)